J Therm Anal Calorim (2018) 131:1491–1497
https://doi.org/10.1007/s10973-017-6553-4

Thermooxidative stability of polypropylene/TiO_2 and polypropylene/layered silicate nanocomposites

Zuzana Cibulková[1] · Anna Vykydalová[1] · Alžbeta Chochulová[1] · Peter Šimon[1] · Pavol Alexy[2] · Leona Omaníková[2]

Received: 24 March 2017 / Accepted: 22 June 2017 / Published online: 3 July 2017

Abstract Thermooxidative stability of polypropylene (PP), PP/TiO_2 and PP/Cloisite 10A nanocomposites was studied using non-isothermal DTA measurements. The effect of various concentrations of both nanofillers on the stability of pristine PP was evaluated. Moreover, the influence of additional processing cycles on the stability of all samples was investigated. For the treatment of the experimental results, our method for the evaluation of the induction periods of thermal oxidation using non-Arrhenian temperature functions was employed. Values of the induction periods were taken as a measure of the samples stability. The results obtained clearly demonstrate that both TiO_2 and Cloisite 10A nanoparticles accelerate thermooxidative degradation of PP. Stability of nanocomposites decreases drastically in comparison with pristine PP, especially at lower concentrations of both nanofillers. The lifetime of all PP samples decreases with additional processing cycles. The steepest decrease is observed after first and second additional passes through the extruder, and then, the stability remains almost constant up to five passes.

Keywords Polypropylene nanocomposites · DTA · Thermooxidative degradation · Induction periods · Titanium dioxide · Layered silicates

Electronic supplementary material The online version of this article (doi:10.1007/s10973-017-6553-4) contains supplementary material, which is available to authorized users.

✉ Zuzana Cibulková
zuzana.cibulkova@stuba.sk

[1] Department of Physical Chemistry, Slovak University of Technology, Radlinského 9, 812 37 Bratislava, Slovakia

[2] Department of Plastics and Rubber, Slovak University of Technology, Radlinského 9, 812 37 Bratislava, Slovakia

Introduction

Polymer nanocomposites consisting of organic polymers and nanofillers are an important class of polymers that have wide application in a number of various industrial sectors. Incorporation of nanofillers leads to improvement of mechanical and physical properties of polymer composites. Thus, polymer nanocomposites have gained wide research interest for developing polymeric materials with improved properties by the incorporation of these nanoscale materials into polymer matrix [1]. Among various nanoscale fillers, layered silicates (such as montmorillonite—MMT) and titania nanoparticles represent the most commonly used ones. Polypropylene (PP) is one of the most commonly used polymers. Due to its low cost, low density, high thermal stability and resistance to corrosion, PP is widely used in many applications, such as fibers, films for food packaging, production of bottles and tubes. PP nanocomposites represent materials with enhanced mechanical properties.

Thermooxidative degradation of PP nanocomposites represents one of the most serious problems, especially at processing. It leads to undesired changes in polymer's physical, mechanical and chemical properties. Although this issue is one of the most important for practice, only few studies deal with this problem. Some studies have reported increased thermal stability of nanocomposites in relation to the pristine PP in the presence of an layered silicate [2–4] and titanium dioxide [5]. On the other hand, very little attention is paid to thermooxidative degradation under the conditions of processing or application. A few papers discuss the effect of the nanofiller on the photooxidative stability of PP/layered silicate composites [6–8]. All studies indicated that layered silicates accelerate the photodegradation of PP, but

do not change its mechanism. Several authors demonstrated that the montmorillonite clay in the PP nanocomposites provides a catalytic effect leading to an acceleration of the material thermal oxidation [9–11]. The effect of TiO_2 nanoparticles on the PP composites thermooxidative stability has been studied in the works of Shawaphun et al. and Manangan et al. [12, 13]. It has been shown that during the polymer processing period, the presence of TiO_2 nanoparticles led to a significant increase in carbonyl index, thus causing acceleration of thermooxidative degradation. Basically, no papers are available dealing with the comparison of the effect of layered silicate and TiO_2 on the thermooxidative stability of PP.

Thermooxidative degradation of materials involves an induction period (IP). At the end of IP, oxidation of the material begins. The end of IP is connected with sudden deterioration of material properties. Therefore, it is often taken as a measure of the material stability [14].

In the present study, the influence of two nanofillers, TiO_2 and organically modified montmorillonite, in PP nanocomposite thermooxidative degradation is evaluated using non-isothermal DTA measurements. Concentration effect of the nanofillers on the thermooxidation of PP matrix is also analyzed. Moreover, the samples under study have undergone additional processing cycles. The effect of PP recycling (represented by additional processing cycles) on the residual stability of pure PP and PP nanocomposites is investigated.

Experimental

Materials

The commercial polypropylene (PP)—Tatren HF 3 22 with a melt flow rate (MFR) of 3 g/10 min (230 °C, 2.16 kg)—was supplied by Slovnaft, a.s. Bratislava, Slovakia. Hombitec S 100 used as a nanofiller was provided by Sachtleben Chemie GmbH, Germany. This type of TiO_2 nanoparticles has a mean diameter of about 15 nm and contains 88% of TiO_2. Cloisite 10A—a benzyl(hydrogenated tallow alkyl)-dimethyl quaternary ammonium-modified montmorillonite from Southern Clay Products, Inc., USA, with a cation exchange capacity of 125 meq/100 g clay and a density of 1900 kg m^{-3}—was used as another type of nanofiller. Both nanofillers were used in 3 different concentrations: 1, 3 and 5 mass%. The samples are denoted as PP (pristine polypropylene), 1C10A (polypropylene with 1 mass% montmorillonite clay), $1TiO_2$ (polypropylene with 1 mass% TiO_2), 3C10A (polypropylene with 3 mass% montmorillonite clay), etc.

Processing

Pure PP and additives were mixed manually and then extruded in a twin screw extruder (LTE 16-40, Labtech, Thailand) with a screw speed of 250 rpm, diameter 16 mm and $L/D = 40$. Temperature profile from hopper to die was 200–210–220–220–220–230–230–220–210–190 °C. After leaving the extruder, the polymer strand was water cooled and cut to granule size of 3 mm.

To simulate the additional processing cycle, the samples were extruded in a single screw extruder Plasticorder Brabender with a screw speed of 30 rpm, $L/D = 25$ and a temperature profile 200–230–220–200 °C. After leaving the extruder, the profile was cooled at an aluminum strand and granulated. This procedure represents one processing cycle and will be denoted as n. The extrusion of all materials was repeated up to five cycles.

Prepared samples can be divided into three main groups:

- Pristine PP
- PP with TiO_2 (1, 3, 5%)
- PP with Cloisite 10A (1, 3, 5%)

Each group consists of undegraded sample and the samples degraded at $n = 1$, 2, 3, 4 and 5. The undegraded samples have passed once through twin screw extruder and will be denoted as PP-0, 1C10A-0, 3C10A-0, $1TiO_2$-0, etc. Degraded samples were obtained from undegraded samples by additional passes through single screw extruder. The samples degraded at $n = 1$ will be denoted as PP-1, 1C10A-1, $1TiO_2$-1, etc.

Scanning electron microscopy

The formation of nanostructures and their distribution in the prepared PP composites was confirmed using scanning electron microscope (JEOL model 7500F). SEM images of the samples can be found in supplementary material (Fig. S1).

DTA/TG measurements

Thermal oxidation of the samples was studied using simultaneous DTA/TG Shimadzu DTG-60. The samples of 2–3 mg were placed in standard aluminum pans. The lid of each pan was perforated by 7 pinholes to enable the contact of the sample with the reaction atmosphere. Oxygen with a flow rate of 50 cm^3 min^{-1} was used as a reaction gas. Each sample was measured at 5 different heating rates: 1, 3, 5, 10 and 15 K min^{-1} in the temperature range of 50–400 °C. The temperature scale was calibrated to the melting point of In, Sn and Zn.

Results and discussion

Treatment of experimental data

From the non-isothermal DTA records, the starting temperatures of oxidation were determined as the onset temperatures of the oxidation peaks. The onset oxidation temperatures (OOT) are summarized in Table 1.

In our previous paper, a method for the evaluation of the induction periods of thermal oxidation using non-Arrhenian temperature functions has been described [14]. The method has been successfully applied to the kinetic description of thermal oxidation of styrene–butadiene rubber in the presence of various antioxidants [15–18], thermooxidative degradation of poppy seeds [19], stabilization effect of antioxidants in ethylene homo- and copolymer [20]. According to this method, for the measurements with constant heating rate, β, the dependence of the OOTs on β can be expressed as [14]

$$T_{\mathrm{i}} = \frac{1}{D}\ln(AD\beta + 1) \quad (1)$$

where A, D are the kinetic parameters describing the length of the induction period. The values of the kinetic parameters enable to calculate the length of the induction period, t_{i}, i.e., the values of the oxidation induction time (OIT):

$$t_{\mathrm{i}} = A\exp(-DT) \quad (2)$$

Dependences of OOTs on the heating rates have been plotted and treated by the nonlinear least square method applying Eq. (1) in the program Origin. The resulting values of the kinetic parameters ln$A$ and D for all samples are listed in Table 2. A very good agreement between the experimental and fitted values of OOT has been achieved for all samples under study and is demonstrated for the samples PP-0, 1C10A-0 and 1TiO_2-0 in Fig. 1. From the values of the kinetic parameters, the lengths of IPs have been calculated for following temperatures: 160, 170, 180 and 200 °C using Eq. (2). Their values are listed in Table 3. The temperatures below 160 °C represent an extrapolation of the obtained data far from the temperature range of measurement with high uncertainties of IP, especially for the case of pure PP. It can be seen that the values of IPs at 200 °C are only several seconds for the experimental conditions applied (very thin layer of melted polymer). Moreover, one has to be careful in the case of predictions for temperatures much below 160 °C since the phase transition (PP melting) takes place. The values of induction periods have been taken as a relative measure of the samples stability.

Effect of nanoadditives on the thermooxidation stability of PP matrix

First, we will discuss the effect of titanium dioxide nanoparticles. As it can be seen from the values of IP,

Table 1 Values of onset oxidation temperatures of the samples under study

n	1 K min^{-1}	3 K min^{-1}	5 K min^{-1}	10 K min^{-1}	15 K min^{-1}
	PP				
0	190.50	201.87	207.85	214.65	221.25
1	188.38	201.19	206.28	215.13	220.26
2	187.26	198.74	206.09	214.47	220.10
3	186.87	198.13	203.23	213.65	218.28
4	185.12	197.11	202.18	210.38	217.78
5	184.11	195.71	200.77	208.84	216.11
	1C10A				
0	182.73	193.30	200.55	207.01	209.35
1	178.05	190.93	196.15	–	208.62
2	178.00	189.68	196.94	204.72	208.67
3	177.95	188.98	195.52	200.78	205.94
4	174.78	189.52	192.49	204.90	207.49
5	171.38	188.53	195.80	200.49	207.62
	3C10A				
0	176.48	184.82	195.40	204.30	208.46
1	169.60	178.94	190.67	192.24	201.73
2	168.34	176.32	185.83	195.31	198.22
3	168.12	176.89	188.89	–	198.15
4	168.03	176.23	182.47	194.40	199.73
5	166.68	172.08	182.75	192.36	196.73
	5C10A				
0	173.13	187.37	193.89	200.56	209.50
1	170.11	178.53	192.76	197.89	209.60
2	165.57	181.39	188.64	194.99	206.65
3	166.15	179.92	189.24	193.16	198.80
4	166.17	180.62	187.63	193.20	199.40
5	166.02	180.02	184.97	189.14	191.91
	1TiO_2				
0	174.40	184.45	193.73	208.92	211.88
1	160.77	172.44	185.23	194.89	198.79
2	–	169.62	181.70	190.12	200.39
3	160.20	167.92	182.77	190.33	199.84
4	164.30	171.96	181.81	188.34	198.48
5	164.60	172.95	181.26	192.32	198.74
	3TiO_2				
0	168.47	175.73	187.38	197.72	210.05
1	157.19	167.22	177.52	193.40	196.65
2	155.56	165.08	175.28	188.85	200.87
3	156.91	164.71	179.82	190.70	198.53
4	154.74	166.14	178.46	191.56	194.90
5	155.81	170.44	172.32	191.53	195.02
	5TiO_2				
0	149.93	167.99	177.09	199.75	204.01
1	145.86	164.14	173.02	185.57	196.27
2	145.74	164.26	170.86	186.95	197.03
3	143.52	164.88	167.88	186.15	192.00
4	145.05	164.54	170.21	188.63	196.21
5	145.04	165.15	167.07	187.38	187.10

addition of TiO_2 to PP caused the decrease in the IP values. It is demonstrated in Fig. 2 that the IPs decreased exponentially with increasing the content of nanofiller. The observed decrease is the most significant for the lowest concentration of 1 mass%, which cut the lengths of IPs to about 20–30% of their original values. Further increase in the TiO_2 concentration led to slower decrease in the PP thermooxidative stability. Similar results have been published in the works of Shawaphun et al. and Manangan et al. [12, 13]. According to their study, TiO_2 can also act as a thermal catalyst during the processing period and induce the auto-oxidation of plastics. They detected significant increase in carbonyl index in PP/nano-TiO_2 films during thermooxidation of these materials. The carbonyl compounds can decompose to more free radicals, thus increasing the oxidation rate.

Addition of C10A nanoparticles to PP also led to lower values of IPs of nanocomposites. Again, an exponential decrease in their lengths with increasing concentration has been obtained (Fig. 2). However, in this case the drop of the stability was less pronounced than in the case of TiO_2. The lengths of IPs in PP containing 1 mass% of C10A were shorter by approx. 50% in comparison with the pristine PP. In both cases, similar trends have been observed for all temperatures and all passes through extruder used. The results presented above clearly demonstrate that the C10A nanocomposites decrease thermooxidative stability of PP.

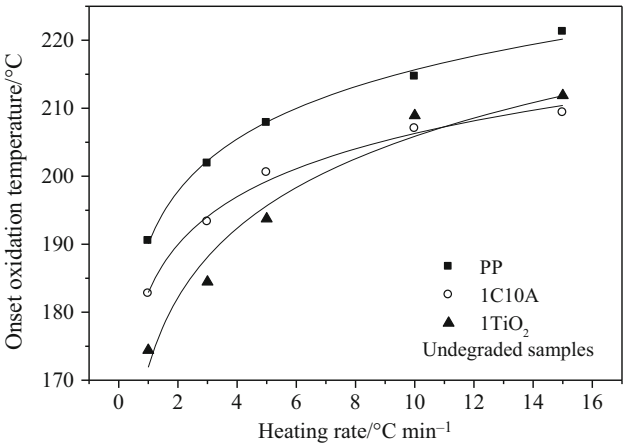

Fig. 1 Experimental and fitted dependences of OOT on heating rate for the samples PP-0, 1C10A-0 and $1TiO_2$-0

Table 2 Values of the kinetic parameters ln*A* and *D*

Sample	ln(*A*)	*D*/K	Sample	ln(*A*)	*D*/K
PP-0	44.1 ± 1.7	0.0900 ± 0.0036	$1TiO_2$-0	32.9 ± 3.2	0.0678 ± 0.0072
PP-1	41.85 ± 0.81	0.0854 ± 0.0017	$1TiO_2$-1	32.1 ± 2.4	0.0679 ± 0.0054
PP-2	40.2 ± 1.3	0.0821 ± 0.0028	$1TiO_2$-2	26.4 ± 2.4	0.0555 ± 0.0055
PP-3	41.6 ± 2.0	0.0853 ± 0.0043	$1TiO_2$-3	31.7 ± 3.8	0.0674 ± 0.0088
PP-4	41.5 ± 2.2	0.0853 ± 0.0046	$1TiO_2$-4	37.7 ± 4.4	0.081 ± 0.010
PP-5	42.1 ± 2.2	0.0869 ± 0.0048	$1TiO_2$-5	36.4 ± 3.5	0.0777 ± 0.0079
1C10A-0	47.2 ± 2.4	0.0984 ± 0.0053	$3TiO_2$-0	31.5 ± 4.4	0.0658 ± 0.0099
1C10A-1	42.52 ± 0.56	0.0889 ± 0.0012	$3TiO_2$-1	30.2 ± 3.1	0.0643 ± 0.0071
1C10A-2	41.6 ± 1.1	0.0868 ± 0.0023	$3TiO_2$-2	28.4 ± 3.5	0.0602 ± 0.0081
1C10A-3	46.5 ± 1.6	0.0979 ± 0.0035	$3TiO_2$-3	29.5 ± 3.5	0.0626 ± 0.0080
1C10A-4	38.9 ± 2.5	0.0813 ± 0.0055	$3TiO_2$-4	29.8 ± 2.4	0.0635 ± 0.0056
1C10A-5	37.1 ± 2.7	0.0775 ± 0.0060	$3TiO_2$-5	31.4 ± 3.6	0.0671 ± 0.0084
3C10A-0	38.7 ± 3.3	0.0808 ± 0.0074	$5TiO_2$-0	23.1 ± 1.8	0.0478 ± 0.0042
3C10A-1	41.0 ± 5.1	0.087 ± 0.012	$5TiO_2$-1	25.8 ± 1.0	0.0548 ± 0.0024
3C10A-2	40.0 ± 3.6	0.0855 ± 0.0080	$5TiO_2$-2	25.3 ± 1.5	0.0535 ± 0.0034
3C10A-3	40.7 ± 5.4	0.089 ± 0.012	$5TiO_2$-3	26.1 ± 1.8	0.0558 ± 0.0054
3C10A-4	39.0 ± 4.0	0.0833 ± 0.0090	$5TiO_2$-4	24.9 ± 1.5	0.0528 ± 0.0035
3C10A-5	41.8 ± 1.9	0.0898 ± 0.0044	$5TiO_2$-5	28.5 ± 3.1	0.0614 ± 0.0073
5C10A-0	34.5 ± 1.9	0.0719 ± 0.0042			
5C10A-1	32.4 ± 3.92	0.0677 ± 0.0085			
5C10A-2	33.3 ± 2.5	0.0699 ± 0.0056			
5C10A-3	39.3 ± 3.1	0.0838 ± 0.0066			
5C10A-4	39.1 ± 1.8	0.0833 ± 0.0041			
5C10A-5	48.9 ± 4.8	0.106 ± 0.011			

Table 3 Lengths of IP calculated for 160, 170, 180 and 200 °C

n	Induction period/min			
	160 °C	170 °C	180 °C	200 °C
	PP			
0	163.2 ± 18	66.4 ± 4.9	27.0 ± 1.0	4.47 ± 0.15
1	128.3 ± 8.8	54.6 ± 2.8	23.25 ± 0.81	4.214 ± 0.043
2	106.8 ± 7.8	47.0 ± 2.1	20.67 ± 0.36	4.00 ± 0.15
3	111 ± 18	46.8 ± 5.4	19.8 ± 1.3	6.50 ± 0.15
4	91 ± 14	38.7 ± 4.3	16.5 ± 1.1	2.995 ± 0.084
5	88 ± 12	37.0 ± 3.2	15.50 ± 0.61	2.73 ± 0.15
	1C10A			
0	97 ± 12	36.4 ± 2.6	13.59 ± 0.24	1.90 ± 0.17
1	55.6 ± 2.4	22.77 ± 0.72	9.36 ± 0.18	1.582 ± 0.073
2	53.52 ± 3.5	22.47 ± 0.95	9.43 ± 0.18	1.662 ± 0.045
3	57.9 ± 5.8	21.8 ± 1.4	8.17 ± 0.24	1.153 ± 0.046
4	41.1 ± 5.3	16.2 ± 1.1	7.440 ± 0.078	1.59 ± 0.14
5	35.1 ± 4.6	18.2 ± 1.4	8.08 ± 0.16	1.58 ± 0.17
	3C10A			
0	41.1 ± 5.9	18.3 ± 1.3	8.168 ± 0.038	1.62 ± 0.25
1	24.4 ± 3.8	10.19 ± 0.42	4.26 ± 0.31	0.74 ± 0.23
2	20.2 ± 1.9	8.59 ± 0.12	3.65 ± 0.24	0.66 ± 0.15
3	22.0 ± 2.9	9.24 ± 0.1	3.88 ± 0.43	0.68 ± 0.24
4	19.1 ± 1.6	8.290 ± 0.071	3.60 ± 0.35	0.68 ± 0.19
5	18.56 ± 0.60	7.56 ± 0.09	3.08 ± 0.17	0.511 ± 0.074
	5C10A			
0	29.8 ± 2.4	14.53 ± 0.56	7.080 ± 0.023	1.70 ± 0.18
1	22.1 ± 5.2	11.2 ± 1.7	5.70 ± 0.37	1.53 ± 0.38
2	20.6 ± 1.2	10.220 ± 0.011	5.08 ± 0.28	1.25 ± 0.19
3	20.7 ± 4.6	8.9 ± 1.4	3.87 ± 0.36	0.75 ± 0.13
4	21.38 ± 0.51	9.30 ± 0.16	4.04 ± 0.23	0.771 ± 0.091
5	19.5 ± 1.2	6.76 ± 0.35	2.34 ± 0.38	0.28 ± 0.10
	1TiO_2			
0	32.6 ± 4.1	16.54 ± 0.87	8.40 ± 0.16	2.16 ± 0.35
1	13.98 ± 0.52	7.09 ± 0.12	3.60 ± 0.25	0.93 ± 0.17
2	10.56 ± 0.50	6.06 ± 0.047	3.47 ± 0.21	1.15 ± 0.20
3	12.00 ± 0.33	6.12 ± 0.37	3.11 ± 0.46	0.81 ± 0.26
4	14.13 ± 0.72	6.29 ± 0.31	2.80 ± 0.42	0.55 ± 0.19
5	14.73 ± 0.87	6.77 ± 0.13	3.11 ± 0.31	0.66 ± 0.17
	3TiO_2			
0	20.4 ± 2.8	10.54 ± 0.39	5.46 ± 0.34	1.46 ± 0.43
1	10.588 ± 0.084	5.57 ± 0.35	2.93 ± 0.39	0.81 ± 0.22
2	9.711 ± 0.012	5.32 ± 0.44	2.91 ± 0.47	0.87 ± 0.28
3	10.620 ± 0.051	5.68 ± 0.43	3.04 ± 0.47	0.87 ± 0.27
4	9.72 ± 0.13	5.15 ± 0.22	2.73 ± 0.27	0.77 ± 0.16
5	9.83 ± 0.22	5.02 ± 0.53	2.57 ± 0.49	0.70 ± 0.28
	5TiO_2			
0	11.309 ± 0.067	7.01 ± 0.29	4.35 ± 0.36	1.67 ± 0.28
1	7.762 ± 0.061	4.49 ± 0.14	2.59 ± 0.14	0.867 ± 0.069
2	7.997 ± 0.045	4.68 ± 0.19	2.74 ± 0.20	0.94 ± 0.10
3	7.10 ± 0.24	4.07 ± 0.31	2.32 ± 0.27	0.76 ± 0.15
4	7.82 ± 0.29	4.61 ± 0.34	2.71 ± 0.29	0.95 ± 0.17
5	6.45 ± 0.45	3.49 ± 0.50	1.89 ± 0.41	0.55 ± 0.20

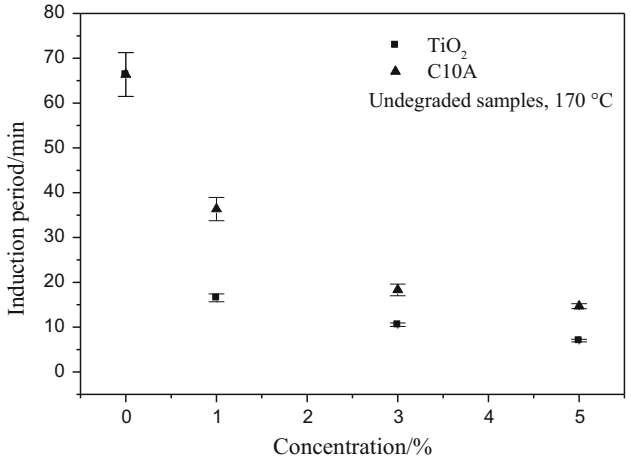

Fig. 2 Dependence of the IP on the concentration of TiO_2 and C10A in PP

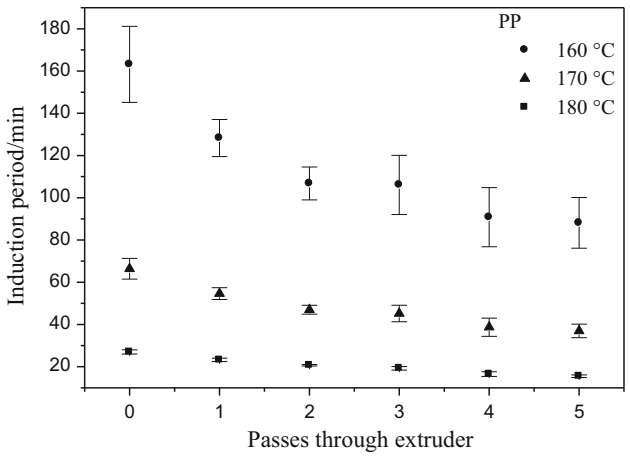

Fig. 3 Dependence of the IP on the passes through the extruder for PP samples

This fact is rarely mentioned in the literature [8–11]. In the few cases, when such results are presented usually the catalytic effect of the silicate is mentioned as the main reason. The most detailed explanation and possibilities were offered by Morlat-Therias et al. [8]. They proposed three possible reasons for the increased thermooxidation of PP nanocomposites. The first one is catalytic effect of heavy metal ions present in the natural silicate clay. It is well known that the transition metal ions, such as iron, display a strong catalytic effect on hydroperoxide decomposition, which is probably the most usual mechanism of filler accelerating effect on polymer oxidation [8]. Another reason is an adsorption of the stabilizers on the surface of the silicate. The third point that should be taken into account is the degradation of the alkylammonium cations used as surfactants. In [7], it has been shown that the photooxidation of organic part of modified montmorillonite produces more radical species and represents a supplementary way to initiate the degradation of the polymer. Another degradation pathway is caused by the decomposition of alkylammonium during processing at high temperature, resulting in a formation of α-olefins [21]. These are sensitive toward oxidation and could participate in the initiation of the polymer degradation. So, the possible prooxidation effect of C10A can be explained either by the presence of transition metal ions, by the adsorption of the stabilizers on the silicate or by the decomposition of alkylammonium cation contained in C10A.

Effect of the additional passes through the extruder

Figure 3 illustrates the effect of the passes through the extruder on the length of the induction period for pure PP samples. It can be seen that the most significant decrease in the stability occurs after the first and the second passes through the extruder. After the second pass, the stability remains almost constant up to five passing cycles. In the case of both nanocomposites (PP/TiO_2 and PP/C10A), the obtained dependences are very similar; again, the highest drop in thermooxidative stability is observable after the first pass through the extruder as it can be seen from the values in Table 3. The effect is similar for all concentrations of nanofillers. Passes through the extruder reduce PP thermooxidative stability less significantly compared to the effect of nanofillers presence in PP, i.e., the IPs of PP thermooxidation after fifth passing cycle reach higher values than those calculated for the addition of both nanofillers.

Conclusions

The results obtained in the study clearly demonstrate that both TiO_2 and C10A nanoparticles accelerate thermooxidative degradation of PP during processing. Stability decreases drastically, especially at lower concentrations of both nanofillers. Increasing amounts of both components leads to exponential decrease in stability of the nanocomposite material. Higher prooxidative effect has been observed for the case of TiO_2. TiO_2 probably acts as thermal catalyst during the processing and causes the autooxidation of PP/TiO_2 composites. The most probable reasons for the decrease in stability of PP/C10A are: the presence of transition metal ions, which display a strong catalytic effect on hydroperoxide decomposition, the adsorption of the stabilizers present in PP and the decomposition of alkylammonium cation contained in C10A. Without additional stabilization, processing of the studied nanocomposites under normal conditions results in products with insufficient durability. Since TiO_2 is used as a photostabilizer and Cloisite 10A to improve the barrier properties of PP, it would be desirable to find the optimal

composition of the stabilizing system to retain the stability of the PP.

The lifetime of all PP samples decreases with the additional passes through the extruder. The steepest decrease was observed after first and second additional passes through the extruder. After the second pass, the thermooxidative stability remains almost constant up to five passes. Comparing the effect of the additional processing cycles and the effect of the nanofillers on the thermooxidative stability of pure PP, it can be concluded that the incorporation of the studied nanofillers decreases the thermooxidative stability of PP more significantly than the additional processing cycles.

Acknowledgements Financial support from the Slovak Research and Development Agency (APVV-15-0124) is gratefully acknowledged.

References

1. Chrissafis K, Bikiaris D. Can nanoparticles really enhance thermal stability of polymers? Part I: an overview on thermal decomposition of addition polymers. Thermochim Acta. 2011;523:1–24.
2. Santos KS, Liberman SA, Oviedo MAS, Mauler RS. Polyolefin-based nanocomposite: the effect of organoclay modifier. J Appl Polym. 2008;46:2519–31.
3. Bertini F, Canetti M, Audisio G, Costa G, Falqui L. Characterization and thermal degradation of polypropylene montmorillonite nanocomposites. Polym Degrad Stab. 2006;91:600–5.
4. Leszczynska A, Njuguna J, Pielichowski K, Banerjee JR. Polymer/montmorillonite nanocomposites with improved thermal properties Part II. Thermal stability of montmorillonite nanocomposites based on different polymeric matrixes. Thermochim Acta. 2007;454:1–22.
5. Esthappan SK, Kuttappan SK, Joseph R. Effect of titanium dioxide on the thermal ageing of polypropylene. Polym Degrad Stab. 2012;97:615–20.
6. Mailhot B, Morlat S, Gardette JL, Boucard S, Duchet J, Gérard JF. Photodegradation of polypropylene nanocomposites. Polym Degrad Stab. 2003;82:163–7.
7. Morlat S, Mailhot B, Gonzalez D, Gardette JL. Photo-oxidation of PP/montmorillonite nanocomposites. 1. influence of nanoclay and compatibilizing agent. Chem Mater. 2004;16:377–83.
8. Morlat-Therias S, Mailhot B, Gonzalez D, Gardette JL. Photooxidation of polypropylene/montmorillonite nanocomposites. 2. Interactions with antioxidants. Chem. Mater. 2005;17:1072–8.
9. Dominkovics Z, Hári J, Fekete E, Pukánszky B. Thermo-oxidative stability of polypropylene/layered silicate nanocomposites. Polym Degrad Stab. 2011;96:581–7.
10. Gutiérre G, Fayolle F, Régnier G, Medina J. Thermal oxidation of clay-nanoreinforced polypropylene. Polym Degrad Stab. 2010;95:1708–15.
11. Fitaroni LB, de Lima JA, Cruz SA, Waldman WR. Thermal stability of polypropylene-montmorillonite clay nanocomposites: limitation of the thermogravimetric analysis. Polym Degrad Stab. 2015;111:102–8.
12. Shawaphun S, Manangan T, Wacharawichanant S. Thermo- and photo-degradation of LDPE and PP films using metal oxides as catalysts. Adv Mater Res. 2010;93–94:505–8.
13. Manangan T, Shawaphun S, Sangsansiri D, Changcharoen J, Wacharawichanant S. Nano-sized titanium dioxides as photocatalysts in degradation of polyethylene and polypropylene packaging. Sci J Ubon Ratchathani Univ. 2010;1(2):14–20.
14. Šimon P, Hynek D, Malíková M, Cibulková Z. Extrapolation of accelerated thermooxidative tests to lower temperatures applying non-Arrhenius temperature functions. J Therm Anal Calorim. 2008;93:817–21.
15. Cibulková Z, Šimon P, Lehocký P, Kosár K, Uhlár J. DSC study of the influence of p-substituted diphenyl amines on the thermooxidative stability of styrene-butadiene rubber. J Therm Anal Calorim. 2010;101:679–84.
16. Cibulková Z, Černá A, Šimon P, Uhlár J, Kosár K, Lehocký P. Stabilization effect of potential antioxidants on the thermooxidative stability of styrene–butadiene rubber. J Therm Anal Calorim. 2011;105:607–13.
17. Cibulková Z, Černá A, Šimon P, Uhlár J, Kosár K, Lehocký P. DSC study of stabilizing effect of antioxidant mixtures in styrene–butadiene rubber. J Therm Anal Calorim. 2012;108:415–9.
18. Černá A, Cibulková Z, Šimon P, Uhlár J, Lehocký P. DSC study of selected antioxidants and their binary mixtures in styrene–butadiene rubber. Polym Degrad Stab. 2012;97:1724–9.
19. Cibulková Z, Čertík M, Dubaj T. Thermooxidative stability of poppy seeds studied by non-isothermal DSC measurements. Food Chem. 2014;150:296–300.
20. Atiqullah M, Cibulková Z, Černá A, Šimon P, Hussain I, Al-Harthi MA, Anantawaraskul S. Effects of supported metallocene catalyst active center multiplicity on antioxidant-stabilized ethylene homo- and copolymers: evaluation of melt stability by nonisothermal DSC study. J Therm Anal Calorim. 2015;119:581–95.
21. Scaffaro R, Mistretta MC, La Mantia FP, Frache A. Effect of heating of organo-montmorillonites under different atmospheres. Appl Clay Sci. 2009;45:185–93.